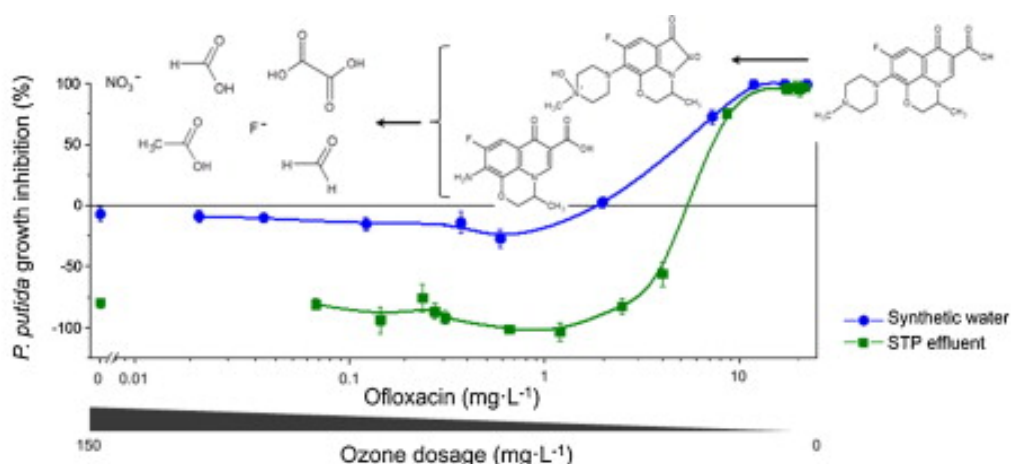


Continuous ozonation treatment of ofloxacin: Transformation products, water matrix effect and aquatic toxicity

Please, cite as follows:

José B. Carbajo, Alice L. Petre, Roberto Rosal, Sonia Herrera, Pedro Letón, Eloy García-Calvo, Amadeo R. Fernández-Alba, José A. Perdígón-Melón, Continuous ozonation treatment of ofloxacin: Transformation products, water matrix effect and aquatic toxicity, *Journal of Hazardous Materials*, Volume 292, 15 July 2015, Pages 34-43, ISSN 0304-3894, <http://dx.doi.org/10.1016/j.jhazmat.2015.02.075>.



Continuous ozonation treatment of ofloxacin: Transformation products, water matrix effect and aquatic toxicity

José B. Carbajo¹, Alice L. Petre^{1,2}, Roberto Rosal^{1,2}, Sonia Herrera^{2,3}, Pedro Letón^{1,2}, Eloy García-Calvo^{1,2}, Amadeo R. Fernández-Alba^{2,3}, José A. Perdígón-Melón^{1,*}

1 Departamento de Ingeniería Química, Universidad de Alcalá, E-28871, Alcalá de Henares, Madrid, Spain

2 Advanced Study Institute of Madrid, IMDEA-Agua, Parque Científico Tecnológico, E-28805 Alcalá de Henares, Spain

3 Department of Chemistry and Physics, University of Almería, E-04120 Almería, Spain

* Corresponding author: ja.perdigon@uah.es

Abstract

The continuous ozonation of the antibiotic ofloxacin (OFX) has been performed using a synthetic water matrix and in a sewage treatment plant (STP) effluent. The aim was to study the effect of the water matrix on the ozonation with particular emphasis on the aquatic toxicity of treated water. OFX was completely removed in both water matrices, although the amount of ozone consumed for its depletion was strongly matrix dependent. The extent of mineralization was limited, and a number of intermediate transformation products (TPs) appeared, twelve of which could be identified. OFX reaction pathway includes the degradation of piperazinyl and quinolone moieties. The further oxidation of TPs gave rise to the formation and accumulation of carboxylic acids, aldehydes, nitrogen-containing organic compounds, and inorganic ions. Aquatic toxicity of treated mixtures was assessed using four standard species: the bacteria *Vibrio fischeri* and *Pseudomonas putida* as target organisms and the algae *Pseudokirchneriella subcapitata* and the protozoan *Tetrahymena thermophila* as non-target organisms. OFX was toxic for the bacteria and the microalgae at the spiked concentration in untreated water. However, the continuous ozonation at the upper operational limit removed its toxic effects. *T. thermophila* was not affected by OFX, but was sensitive to STP effluent.

Keywords: Quinolone antibiotic; Continuous ozonation; Reaction pathway; STP effluent; Biotest battery.

1. Introduction

Antibiotics are commonly used to treat infections in humans and are intensively applied for veterinary uses [1]. As a consequence of their poor metabolization and their incomplete removal in sewage treatment plants (STPs), antibiotics are continuously released into the aquatic environment [2] and [3]. Their occurrence in surface waters has generated human health and environmental concerns. Although found at sub-therapeutic levels, relatively low concentrations of these drugs can promote bacterial resistance [4] and [5]. Indeed, antibiotic resistant bacteria (ARB) and antibiotic resistance genes (ARGs) have been found in STP effluents, surface, and drinking waters [6] and [7]. Despite the fact that antibiotics are specifically applied to fight pathogenic bacteria, non-target environmental organisms which provide important ecosystem services are inevitably exposed, resulting in a potential risk of ecosystem disruption [1] and [8].

Ofloxacin (OFX), a quinolone, is a broad-spectrum antibacterial agent widely used for treating bacterial infections [9]. In conventional STP, OFX is partially removed (apparent removal efficiency of 60%), mainly by adsorption onto activated sludge [10] and [11], being

the balance discharged with treated wastewater. In fact, OFX has frequently been detected in STP effluents and river basins in up to $\mu\text{g L}^{-1}$ and ng L^{-1} levels, respectively [3], [11], [12] and [13]. As a consequence of its occurrence and toxicity, recent publications have concluded that OFX might pose a substantial risk to aquatic organisms [12], [14], [15] and [16].

As conventional processes used in STP are unable to act as a reliable barrier toward some pharmaceutical compounds, a great effort is currently directed to develop technologies capable of efficiently removing them [17]. Among them, ozonation is known as an attractive alternative due to its effectiveness in the removal of a wide range of micropollutants with potential environmental risks [18], [19], [20] and [21]. A further advantage of the ozonation is its disinfecting potential, which is able to deactivate ARG biological activities in addition to achieving ARB inactivation, preventing the dissemination of antibiotic resistance [22] and [23].

Using continuous processes working with real STP effluents have proven more useful than batch/semi-batch works performed in wastewater or simulated effluents for full-scale studies. Continuous treatment displays a closer approximation to a full-scale system and a better

understanding of the fate of pollutants under oxidizing conditions [19]. In addition to the reaction time and ozone dose, the extent of oxidation depends mainly on the chemical nature of the micropollutant itself and water matrix composition [24]. Moreover, it is important to take into account that the abatement of the target compound rarely leads to its total mineralization, but rather the formation of transformation products (TPs). The concern is whether or not these TPs keep the biological effects of the parent compounds or whether new and undesired biological effects are developed [25], [26], [27] and [28]. This issue cannot be addressed merely elucidating the structures of the TPs by chemical analysis. Instead, the assessment of treated water toxicity and the influence of the water matrix are necessary for the optimization of continuous ozonation treatments.

In this work, the continuous ozonation of OFX in two different water matrices (synthetic water and STP effluent) was studied, elucidating its TPs in order to propose a reaction pathway. Aquatic toxicity of treated water was assessed using a biotest battery composed of two target (*Vibrio fischeri* and *Pseudomonas putida*) and two non-target (*Pseudokirchneriella subcapitata* and *Tetrahymena thermophila*) organisms.

2. Materials and methods

2.1 Materials

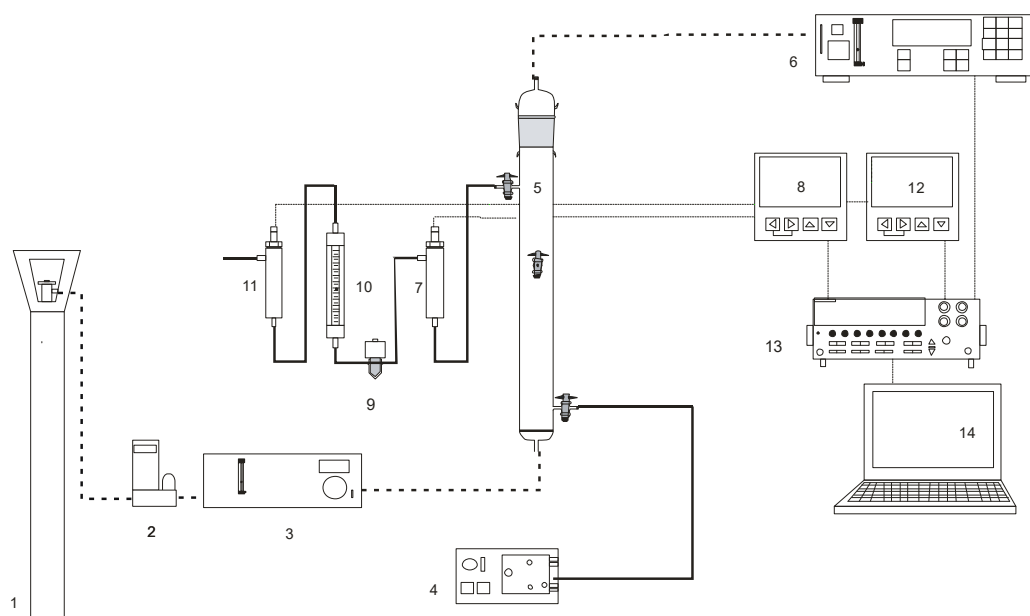
Ofloxacin (OFX) was purchased from Sigma–Aldrich ($\geq 98\%$). Two water matrices spiked with OFX (22 mg L^{-1}) were used for ozonation process experiments: synthetic water and a STP effluent. The synthetic matrix was prepared in ultrapure water (resistivity $\geq 18\text{ M}\Omega\text{ cm}$ at 25

$^{\circ}\text{C}$) with the required amount of sodium bicarbonate to equal the alkalinity and pH values of the STP effluent. Wastewater was collected from the outlet of the secondary clarifier of a STP located in Alcalá de Henares (Spain). The plant treats domestic wastewater with a minor contribution of industrial effluents from facilities located near the city and has a nominal capacity of $3000\text{ m}^3\text{ h}^{-1}$. Details on wastewater characterization are included as Supplementary data (Table S1).

2.2 Experimental procedure

The experiments were carried out in a cylindrical reactor (internal diameter of 6.0 cm and working height of 51 cm) with a total working volume of 1.44 L, which operated in continuous co-current mode (Scheme 1). The retention time distribution curve yielded an average retention time of 10.3 min. The reactor modelling using the continuous stirred tank reactor (CSTR) in series model [29] determined an equivalent value of 1.13 tanks, indicating that the bubble column can reasonably approach a perfect CSTR [30].

Water flow rate was 142 mL min^{-1} and gas flow was 390 mL min^{-1} with different inlet ozone concentrations. During the runs, the inlet ozone dosage was stepwise increased from 4.2 to 145 milligrams of ozone per litre of wastewater (mg L^{-1}). For the different ozone dosages samples were withdrawn for analysis at the column outlet once the stationary state was reached. This was ensured by circulating the hydraulic retention time four times after a constant ozone concentration was obtained both in liquid and gas phases at the column outlet. Assuming CSTR behaviour and stationary state ($d\text{CO}_{3,\text{liq}}/dt=0$), the



Scheme 1. Experimental set-up. 1. Oxygen cylinder, 2. Mass flow controller, 3. Ozone generator, 4. Peristaltic pump, 5. Bubble column, 6. Ozone gas analyser, 7. Dissolved ozone sensor, 8. Dissolved ozone transmitter, 9. Needle valve, 10. Rotameter, 11. pH sensor, 12. pH transmitter, 13. Data acquisition system, 14. Computer. Water line is represented as solid line, gas line as dotted line and electrical wiring as dashed line.

amount of ozone consumed can be obtained by means of the following mass balance (Eq. (1)):

$$\text{Consumed } O_3 = F_{O_3}^{\text{gas,in}} - F_{O_3}^{\text{gas,out}} - F_{O_3}^{\text{liq,in}} \quad [1]$$

in which F_{O_3} is the rate of ozone entering the system in the gas phase (gas, in) or leaving either in the exhaust gases (gas, out) or dissolved in water (liq, out). Details are given in Supplementary data.

2.3. Analytical methods

OFX concentration was performed by HPLC (Agilent 1200) and the structural elucidation of TPs was carried out using a hybrid quadrupole time-of-flight mass spectrometer TripleTOF 5600 system (AB SCIEX) with an ESI (electrospray ionization) source coupled to an Agilent 1200 Series HPLC system (LC/ESI-QTOF-MS). DOC was determined using a TOC-VCSH Shimadzu TOC analyser. Carboxylic acids were measured by a Dionex DX120 IC and inorganic ions were determined by means of a Metrohm 861 Advance Compact IC. Formaldehyde was measured using acetylacetone method (Hach-Lange LCK 325). Analytical methods are detailed in Supplementary data.

2.4. Aquatic toxicity bioassays

Aquatic toxicological assessment was performed with a bioassay battery composed of the standard single species tests of the bacteria *V. fischeri* and *P. putida*, the algae *P. subcapitata* and the protozoan *T. thermophila*. This set of bioassays allowed both acute and chronic assays to be performed and the combined usage of target (prokaryotes) and non-target (eukaryotes) OFX organisms at different trophic levels. All these bioassays were conducted according to standard operational guidelines [31], [32], [33] and [34]. Supplementary data shows more details about the aquatic toxicity test procedures.

3. Results

The continuous ozonation process was studied from different ozone dosages in order to achieve maximum OFX oxidation and mineralization degrees.

3.1 Synthetic water matrix

Fig. 1 shows the evolution of OFX concentration and DOC in the synthetic matrix as a function of the amount of ozone supplied. OFX declined with ozone up to an exposure of 60 mg L⁻¹, where it was completely removed. Otherwise, despite DOC also decaying with ozone, ozonation did not lead to OFX mineralization, with maximum values slightly over 40 %.

The evolution of the consumed and dissolved ozone is also represented in Fig. 1. Based on the evolution of both parameters, three different zones can be observed as a function of ozone dosage. In zone 1, up to 58 mg L⁻¹, ozone consumption linearly increased, and no dissolved ozone was detected (<0.01 mg L⁻¹), which indicated that ozone was acting as limiting reactant. This behavior

occurred during the oxidation of more easily oxidizable compounds because ozone mass transfer rate was slower than ozone consumption. In this initial zone, total OFX degradation was reached, suggesting that the target pollutant is easily abated by ozonation. This result was in line with previous studies using semi-batch processes. Márquez et al. [35] reported high second-order rate constants (>106 M⁻¹ s⁻¹) at pH >7 and De Witte et al. [36] found a half-life time of 12.8 min at pH 7 for ozone inlet of 0.58 mg min⁻¹. Runs carried out using t-butanol (30 mM) as a radical scavenger (Fig. S1, Supplementary data) suggest that OFX is mainly degraded by molecular ozone attack. The direct ozonation reaction would occur with the fast reacting moieties present in the OFX molecule such as the deprotonated amine and the aromatic ring (103–1011 M⁻¹ s⁻¹) [35], [36] and [37]. Dodd et al. [38] also observed that the kinetics of other quinolone reactions was predominantly driven by molecular ozone oxidation.

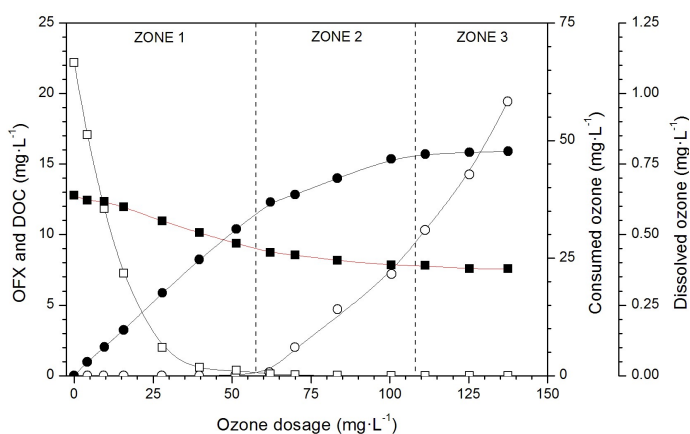


Figure 1. Evolution of ofloxacin (OFX) (□), DOC (■), consumed ozone (●) and dissolved ozone (○) at different ozone dosages in synthetic water matrix.

The DOC depletion achieved in zone 1 was 30 %, which represented roughly three quarters of the maximum mineralization degree achieved along the runs. In zone 2, consumed ozone still increased and dissolved ozone began to be detected at the outlet stream. This fact is consistent with the oxidation of less easily oxidizable compounds, whose ozonation proceeded at a slower rate than ozone mass transfer. In this zone, the mineralization degree slightly rose from 30 to 41%, suggesting that the increase of consumed ozone was mainly due to the partial oxidation of organic matter. For dosages above 108 mg L⁻¹ (zone 3), ozone consumption remained constant, without further mineralization and a concentration of ozone at the reactor outlet (gas and liquid) which increased proportionally to ozone input. Under these conditions, the upper operational limit of the system, the consumed ozone value was 48 mg L⁻¹. Taking into account both consumed ozone and the abatement degree of OFX at the upper ozone dosage, the ozone consumed per milligram of OFX found in the synthetic water matrix was 2.15 mg O₃ (mg OFX)⁻¹. Considering the ozone

consumed by the matrix (Fig. S2, Supplementary data), the mass factor was $2.02 \text{ mg O}_3 (\text{mg OFX})^{-1}$.

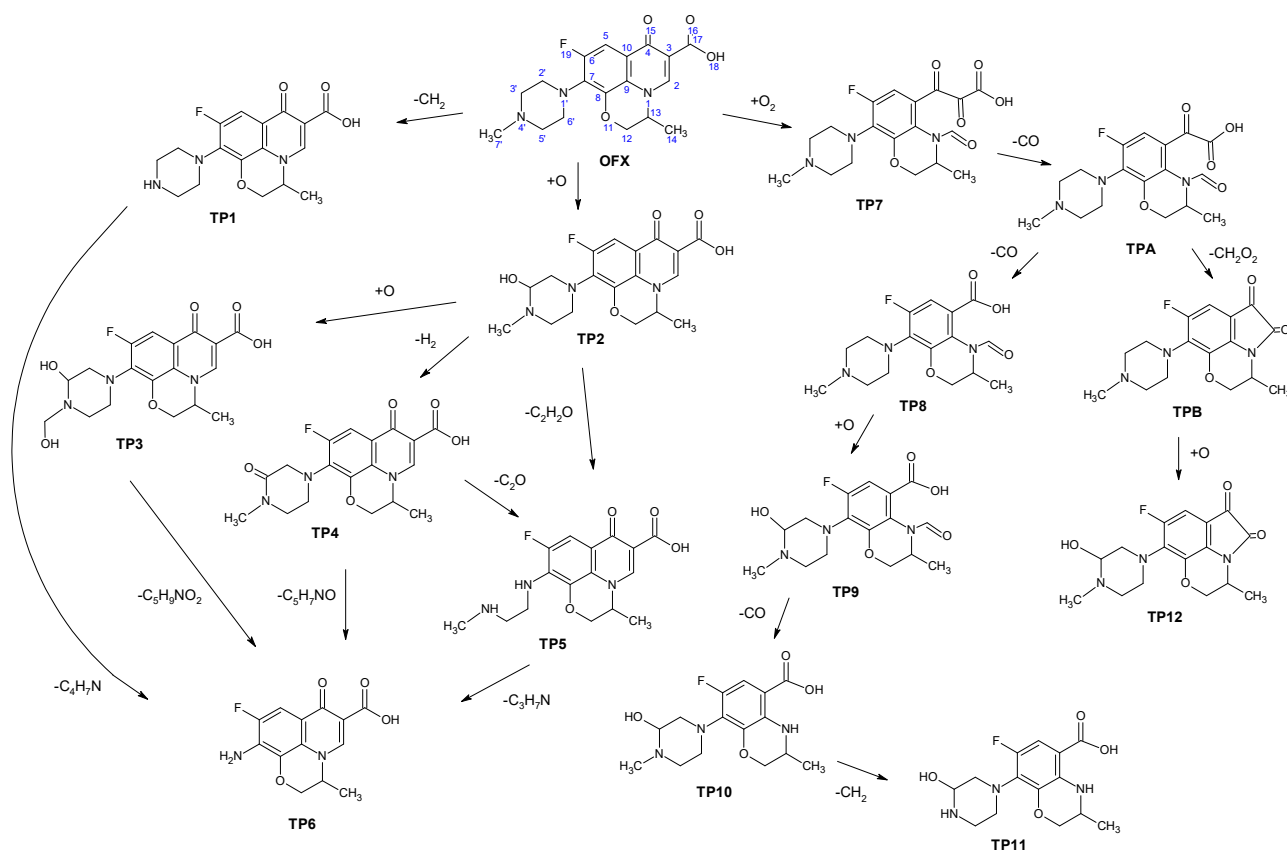
3.2 Elucidation of transformation products and degradation pathway

Twelve compounds were elucidated as TPs formed during the ozonation of OFX (Supplementary data Table S2). The evolution of the corresponding TPs and OFX depletion as a function of the amount of ozone supplied are shown in Fig. 2. Relative amounts were calculated from the ion counts associated with each individual compound normalized by the ion count corresponding to the initial concentration of OFX. This approach allowed the yields and the evolution of TPs to be estimated, while their actual concentrations could not be determined due to the lack of standards [39]. As can be seen in the figure, the TP amounts behaved as an intermediate product in series reactions, with their counts initially increasing to reach a maximum and then decreasing due to the further oxidation of these products by ozone. In fact, the maximum concentration of most TPs occurred for ozone dosages between 4.2 and 28 mg L^{-1} , and all of them disappeared at ozone exposure of 64 mg L^{-1} (at the end of zone 1), demonstrating thus their high reactivity with ozone (Fig. 2A). It is worth mentioning that the yields of TPs were variable, with the highest ion counts corresponding to TP2.

The generation pathway of these TPs is expected to include multiple routes due to the presence of several reactive sites in the parent compound and the occurrence of two oxidation mechanisms by both molecular ozone

and hydroxyl radicals. Despite this complexity, the results presented above and the information available from reported data [36] and [39] can be interpreted to propose the degradation pathway shown in Scheme 2. The degradation of OFX occurs on both piperazinyl (TP1–TP6, open symbols in Fig. 2) and quinolone ring (TP7–TP12, solid symbols in Fig. 2). No TPs were found corresponding to the degradation of the oxazinyl group, indicating that it remained unmodified by ozonation reactions.

On the one hand, the reactions of the piperazinyl ring were due to attacks to both the methyl group and the piperazine core. TP1 is attributed to the demethylation of the piperazinyl ring at position 4'. TP1 could be regarded as one of the intermediates for the formation of TP6, which can be yield owing to the total oxidation of the piperazine ring to an amino group. The main transformation product TP2 was a consequence of the initial ozone attack on N4' atom [38]. The oxidation of TP2 may yield TP3 through the addition of a hydroxyl radical at 7'. OFX can also be oxidized to the keto-derivative TP4, which would be transformed into TP5 through the opening of the piperazine ring. Further oxidation of TP3 and TP5 would generate TP6. These cited TPs, from the reaction of the piperazine group, seem to be formed primarily via molecular ozone attack [39]. According to the proposed reaction pathway, the carbonyl and carboxyl groups at the quinolone moiety, which are essential for binding at the DNA gyrase [9], were not modified in TP1–TP6 so the direct ozonation



Scheme 2. Proposed degradation pathway for ofloxacin (OFX) in ozonation process.

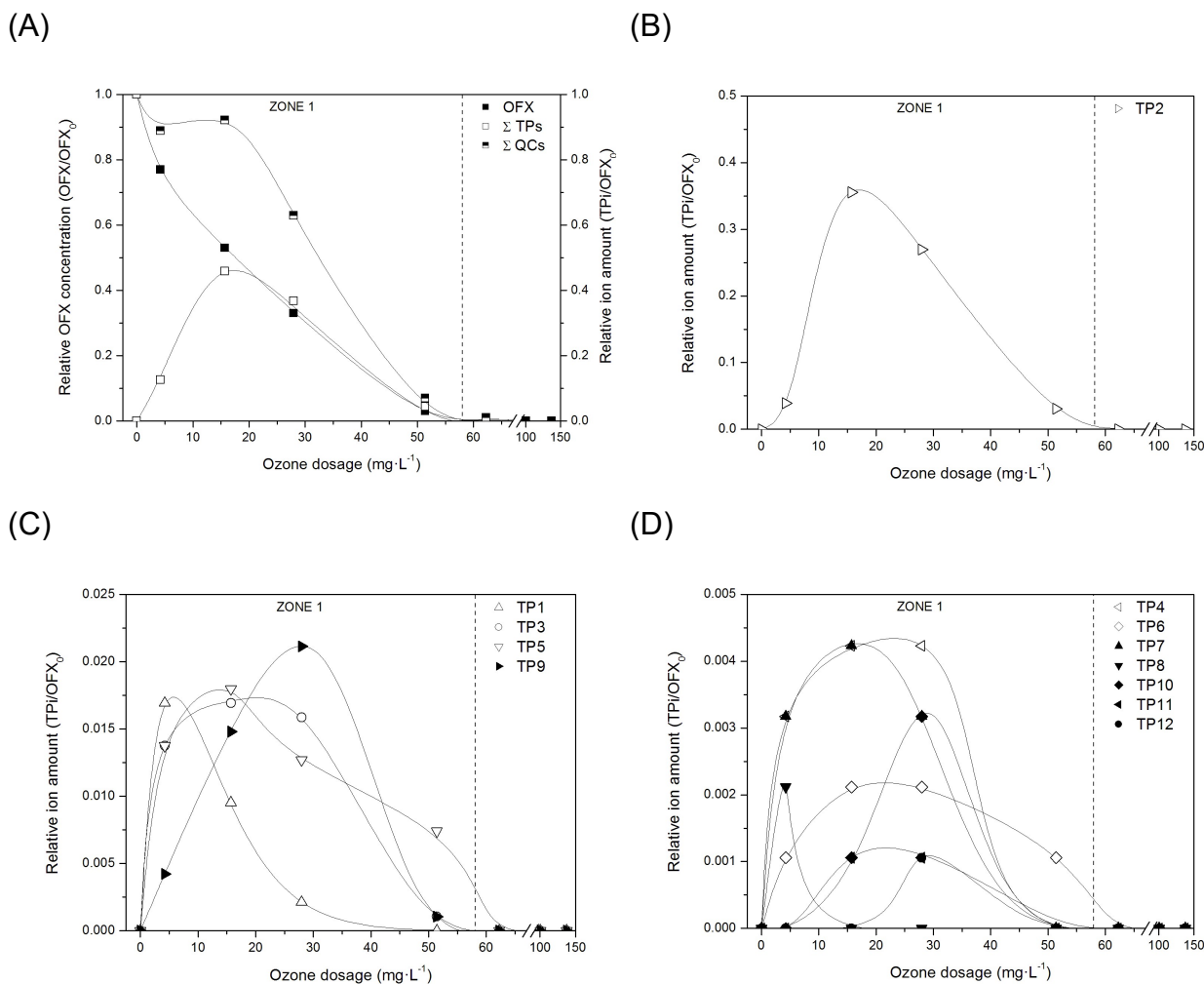


Figure 2. Evolution of ofloxacin (OFX), transformation products (TPs) and quinolone core compounds (QCs) at different ozone dosages in synthetic water matrix.

mechanism is not likely inactivating the drug. Under this assumption, the sum of ion counts from TP1–TP6 and OFX, would correspond to biologically active compounds, non-monotonically decreased up to ozone dosages higher than 16 mg L⁻¹ as observed in Fig. 2A. On the other hand, the oxidation of quinolone moiety through the breaking of C₂=C₃ double bond led to TP7. In agreement with Liu et al. [39], TP7 should produce TPA (non-observed in the present study), whose decarboxylation at C₃ yields anthranilic acid analogues (TP8–TP11), whereas deformylation at C₂ leads to isatin analogue formation (TPB and TP12). TPs from reactions at the quinolone moiety were a consequence of hydroxyl radical reactions according to reported data on fluoroquinolone degradation [36] and [39]. The proposed degradation pathway for the early oxidation stages of OFX is not only consistent with the evolution and yield of TPs, but also supports that OFX oxidation was most likely due to direct ozonation reactions. In fact, TPs from reactions at piperazine group, mainly generated by molecular ozone (open symbols in Fig. 2), were more abundant than those at quinolone moiety, primarily consequence of radical reactions (full symbols in Fig. 2).

Fig. 3 represents the evolution of the main detected carboxylic acids (mesoxalic, oxalic, acetic, and formic

acid) found in ozonation runs. Their concentration increased in zone 2 due to the partial oxidation of organic matter. This explains the noticeable increase of consumed ozone in spite of OFX has been completely depleted. In zone 3, the concentration of carboxylic acids remained essentially constant together with mineralization degree. This fact is in good agreement with the well-known refractory character of these final ozonation products, which is the reason why their concentrations increased in the reaction mixture [40] and [41]. The organic acids only account for a third of DOC. As a consequence, other refractory organic compounds were not detectable by ionic chromatography, such as aldehydes or nitrogen-containing organic compounds, which should be present [42]. Among aldehydes, formaldehyde was detected at a concentration close to 1.0 mg L⁻¹ at ozone exposures of 39 mg L⁻¹, probably as a result of the reaction yielding TPs such as TP1.

Nitrogen was not completely mineralized as shown by the amount of nitrate detected, which achieved a maximum value corresponding to 30% of the initial nitrogen content of OFX (11.3 mg L⁻¹). This fact suggests that the remaining organic carbon contained a high amount of nitrogen in compounds such as quaternary amines which are species that are particularly

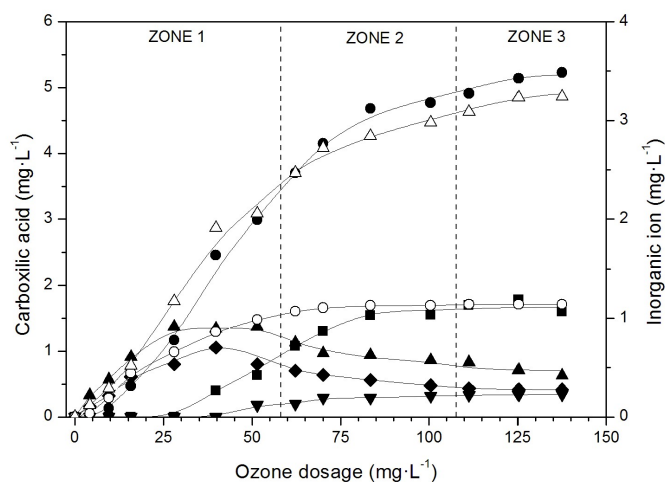


Figure 3. Evolution of formaldehyde (◆), mesoxalic (■), oxalic (●), acetic (▼) and formic acid (▲) and nitrate (Δ) and fluoride (○) at different ozone dosages in synthetic water matrix.

refractory to ozonation [43] and [44]. OFX decay also led to the occurrence of other inorganic ion, fluoride, whose concentration reached a value corresponding to 100% initial fluorine in OFX.

3.3 Matrix effect

STP effluent showed an instantaneous ozone demand of 8.7 mg L⁻¹, in line with reported values for other wastewaters [45] and [46]. The organic compounds (DOC = 8.4 mg L⁻¹) were mineralized at an extent of 20% at the upper operational condition, consuming 18 mg O₃ L⁻¹ (Fig. S2). Fig. 4A represents the evolution of OFX, DOC and the concentration profiles for consumed and dissolved ozone during the ozonation of OFX in STP effluent. A new zone, denoted zone 0, was identified for ozone dosages lower than 16 mg L⁻¹. In it, OFX was only slightly oxidized, with a depletion of about 20%, whereas in synthetic water matrix for similar ozone exposures it reached 67%. On the contrary, DOC steeply decreased

quickly achieving a mineralization degree of 16%. These data show the competition for ozone between the dissolved organic compounds of the water matrix and OFX, suggesting that ozone/hydroxyl radicals would preferably attack certain moieties in wastewater organic matter. This fact is in line with Katsoyiannis et al. [24], who showed that the kinetics of the reaction of ozone with DOC strongly affects the rate at which target compounds were transformed by ozone. Beyond this preliminary zone, a similar profile to synthetic matrix was observed. In zone 1, OFX was almost completely abated, and DOC fell steadily down to 16 mg L⁻¹ (28%) with increasing ozone exposure up to 84 mg L⁻¹. In zone 2, between 84 to 124 mg L⁻¹, ozone consumption increased, and the mineralization degree slightly rose from 28 to 33% (DOC = 15 mg L⁻¹). Further ozone dosage up to 124 mg O₃ L⁻¹, did not increase mineralization and the amount of ozone consumed remained constant at 64 mg L⁻¹. As a result, this value was considered the upper operational limit.

The evolution of individual carboxylic acids and inorganic ions with ozone dosage is displayed in Fig. 4B. The pattern of organic acids was similar to that found in synthetic water matrix for zones 1–3. However, higher concentrations were detected at the upper operational limit due to the partial oxidation of wastewater organic matter [42]. The nitrate concentration was significantly higher than that found in synthetic matrix, reasonably as a consequence of the oxidation of ammonium and nitrite present in the STP effluent. Nitrite reacts rapidly with ozone and is almost stoichiometrically oxidized to nitrate [40]. This reaction took place in zone 0 at low ozone dosage (Fig. 4B). Taking into account the nitrate from wastewater matrix, OFX nitrogen mineralization was around 25%, value close to the observed in the synthetic water. Fluoride represented a value close to 100% of the fluoride in the structure of OFX and was not detected in zone 0 in which a low OFX depletion took place.

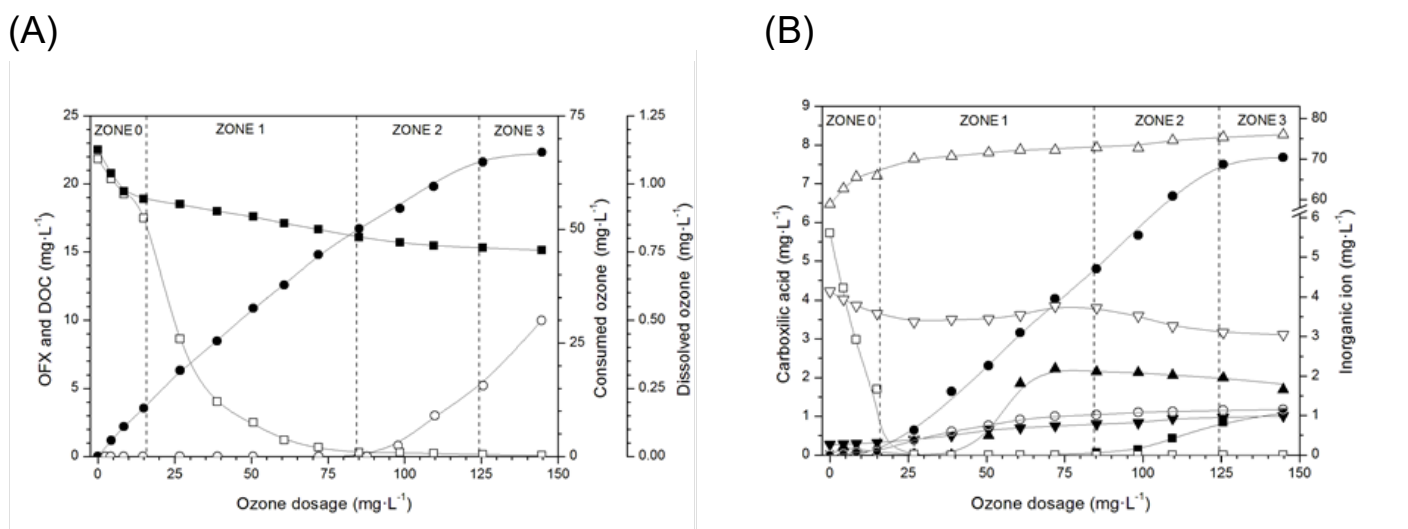


Figure 4. (A) Evolution of ofloxacin (OFX, □) DOC (■), consumed ozone (●) and dissolved ozone (○). (B) Profiles of mesoxalic (■), oxalic (●), acetic (▼), formic acid (▲), nitrate (Δ), nitrite (□), ammonium () and fluoride (○) at different ozone dosages in STP effluent.

The total abatement of OFX was reached for an ozone dosage of 85 mg L^{-1} , which was considerably higher than that observed in the synthetic water matrix (60 mg L^{-1}). The maximum ozone consumption was 64 mg L^{-1} , which was also higher than the value obtained in synthetic water (48 mg L^{-1}) and close to the sum of ozone consumed by the wastewater matrix, 18 mg L^{-1} (Fig. S2), and that due to OFX abatement, 45 mg L^{-1} (Fig. 1). The ozone dose in STP effluent was $2.95 \text{ mg O}_3 (\text{mg OFX})^{-1}$, which was remarkably higher than that observed in synthetic water ($2.15 \text{ mg O}_3 (\text{mg OFX})^{-1}$). Fig. 5 displays the evolution of ozone consumption as a function of OFX removed in both matrices. In the synthetic water matrix, the amount of ozone consumed increased steadily with OFX removed (zone 1) with a sharp rise at the highest values as a consequence of the reactions of ozone with partial oxidized organic matter (e.g., carboxylic acids), which are mainly occurred in zone 2. On the other hand, in the real wastewater matrix, the ozone consumed rose relatively quickly up to $12 \text{ mg O}_3 \text{ L}^{-1}$, for low OFX abatement. Subsequently, the profile of consumed ozone of both water matrices runs almost in parallel. The ozone consumption gap between both matrices matches with the amount consumed by the STP effluent in the previously defined zone 0. In this preliminary zone, ozone is primarily consumed by reactions with the dissolved organic matter in wastewater (8.4 mg L^{-1}), part of which was easily oxidizable at low ozone dosages [47], and the oxidation of reduced nitrogen species.

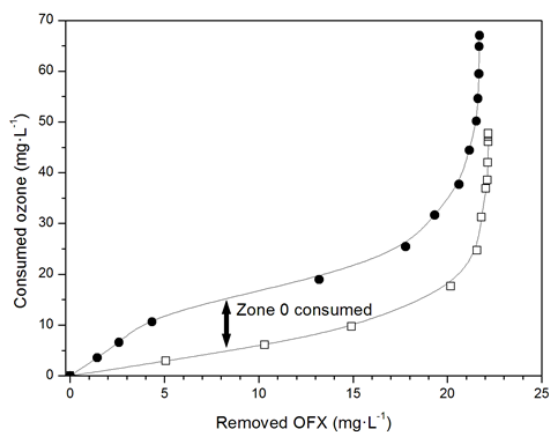


Figure 5. Evolution of ozone consumption throughout ofloxacin (OFX) abatement in synthetic water matrix (□) and STP effluent (●).

Total OFX depletion did not lead to its full mineralization in the real matrix either, achieving a maximum DOC removal of 33%. Because OFX was not the only organic compound in the spiked STP effluent and taking into account that the maximum amount of organic carbon mineralized in wastewater was 1.9 mg L^{-1} (Fig. S2), the OFX mineralization degree for maximum ozone dosages was 24%, significantly less than the 41% obtained in synthetic water. These facts underline that OFX oxidation and mineralization degrees were not only influenced by the presence of naturally occurring radical scavengers (mainly carbonates and bicarbonates), but

also by other inorganic and organic compounds which hamper its depletion and mineralization through indirect reactions [24] and [47].

3.4 Aquatic toxicity assessment

First, the toxicity of OFX on single species was evaluated by determining concentration-response curves (see Supplementary data Fig. S3). The growth inhibition assay with *P. putida* test was the most sensitive with an EC_{50} value of 0.11 mg L^{-1} . This is a consequence of the specific design of quinolone, which inhibits bacterial cell division [9]. *P. subcapitata* also presented a low EC_{50} value, 1.9 mg L^{-1} , although microalgae are non-target organisms for the antibiotic. Nevertheless, it has been indicated that the presence of gyrase-like proteins makes algae sensitive to OFX and warns about the effect of quinolone on non-target organisms [8]. On the other hand, *T. thermophila* and *V. fischeri* have EC_{50} values $>100 \text{ mg L}^{-1}$. *T. thermophila*, a eukaryote, is not expected to be affected by antibiotics [8], whereas *V. fischeri*, despite being a target organism, was not OFX sensitive due to the short incubation time of the bioassay [48]. The EC_{50} values were in good agreement with those previously reported for *V. fischeri*, *P. putida* and *P. subcapitata* [16] and [49]. No prior data have been found for *T. thermophila*.

Fig. 6 displays the evolution of the toxicity of untreated and treated samples at different ozone exposures in the synthetic water matrix and STP effluent for the organisms of the bioassay battery. The aquatic toxicity of raw synthetic water ($\text{OFX} = 22 \text{ mg L}^{-1}$) displayed significant interspecies differences, which essentially correspond to the already described sensitivity to OFX. Accordingly, the growth of *P. putida* and *P. subcapitata* was severely inhibited as quinolone concentration was considerably higher than EC_{50} values. The lower effect on *V. fischeri* and *T. thermophila* was consistent with their lower sensitivity to OFX. A similar behaviour was observed for spiked STP effluent on all bioassays except for *T. thermophila*, whose toxicity was markedly higher. This fact is result of the toxicity of the STP effluent itself. In contrast, the wastewater matrix did not display noticeable toxicity for the rest of bioassays.

In the synthetic water matrix, the toxicity for *P. putida* and *P. subcapitata* was reduced with the increasing ozone dosage up to its total depletion. At the end of zone 1, aquatic toxicity for both microorganisms reached the same value of the non-spiked synthetic water. The toxic effects for *V. fischeri* increased with ozone exposure at low ozone dosage, whereas for *T. thermophila* no growth inhibition was observed in any case. The toxicity for *V. fischeri*, *P. putida* and *P. subcapitata* in STP effluent, decreased with increasing ozone dosage until the inhibition value of control sample was reached. The toxic effects for *T. thermophila* follow a similar trend to the non-spiked wastewater profile throughout all input ozone levels, suggesting that ozonated STP effluent appeared to be the main source of toxicity to the protozoan.

SYNTHETIC WATER MATRIX

WASTEWATER MATRIX

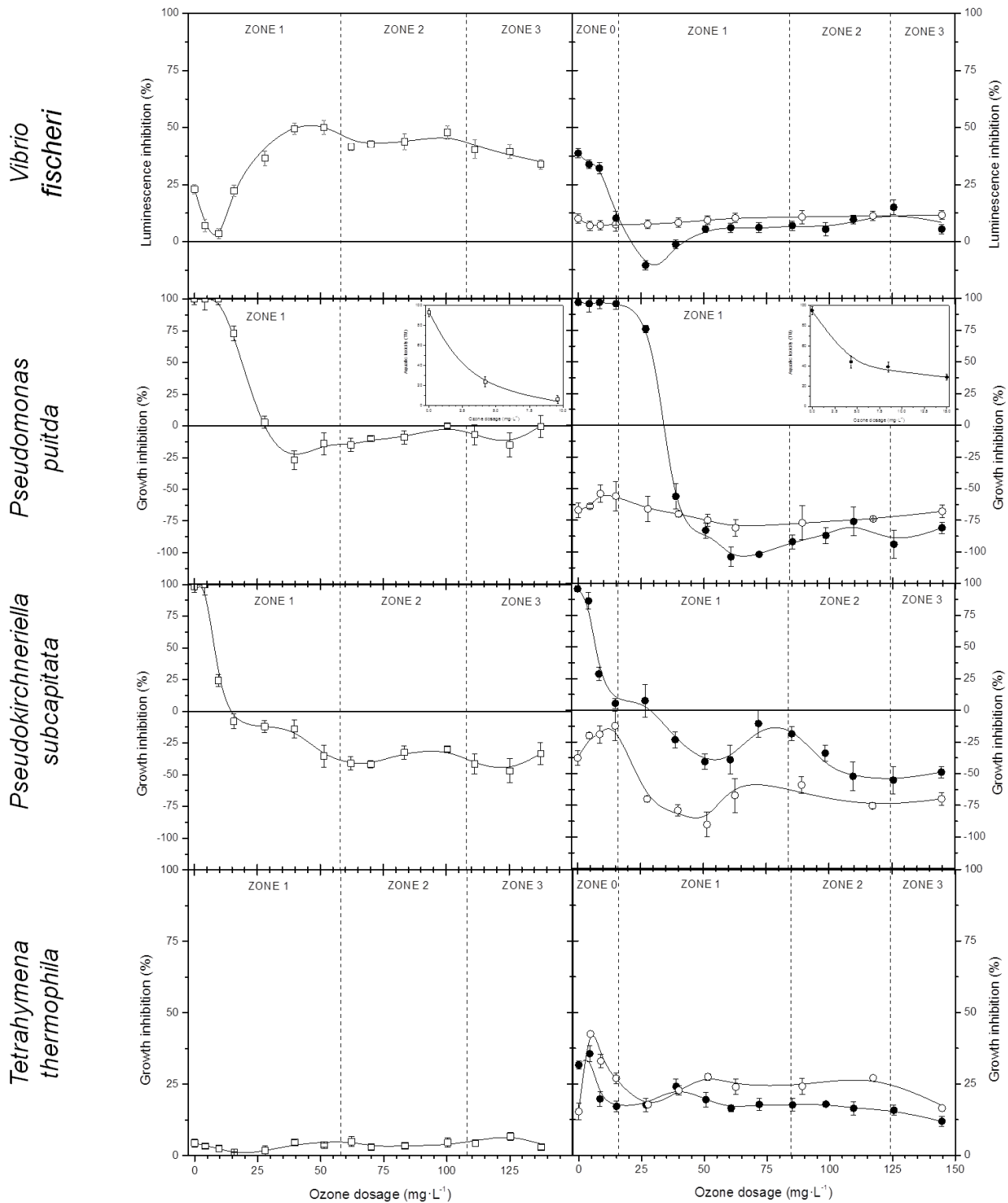
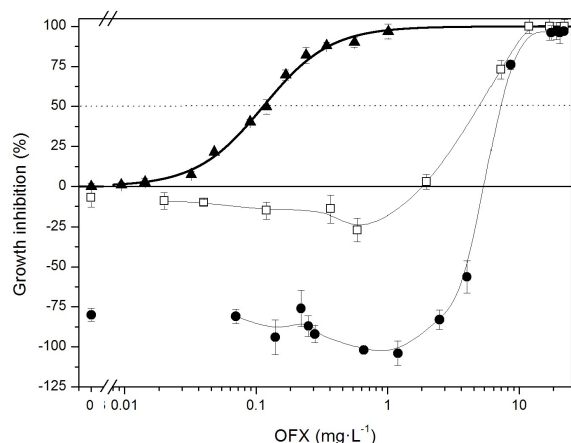


Figure 6. Evolution of the effects of treated samples at different ozone dosages in ofloxacin spiked synthetic water (□) and STP effluent (●) and non-spiked STP effluent (○) on biotest battery (Mean ± 95% Confidence Interval).

Aquatic toxicity and OFX concentration followed a similar profile with increasing ozone dosage, both being completely depleted at the end of zone 1. Toxicity decay in wastewater matrix required a higher amount of ozone with regards to the synthetic water matrix. In general, it can be observed that the toxicity did not significantly

decay in zone 0 in the STP effluent where OFX depletion was slowed down by matrix effects. Fig. 7 shows a comparison between toxic effects of pure OFX dissolved in ultrapure water and that exerted by ozonated solutions of OFX in two different water matrices on the most sensitive organisms: *P. putida* and *P. subcapitata*.

(A)



(B)

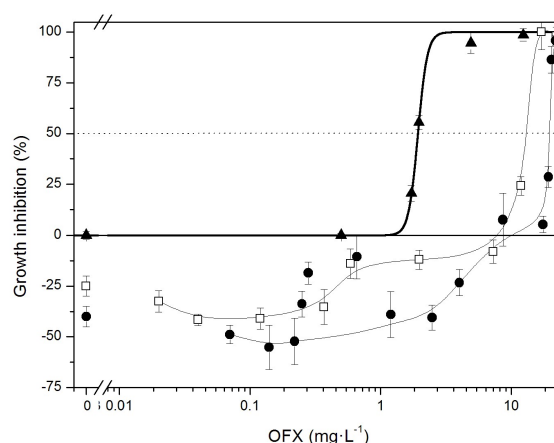


Figure 7. Concentration-response curve of single ofloxacin (▲) and evolution of the effects of treated samples at different remaining ofloxacin (OFX) concentration in ozonated synthetic water matrix (□) and wastewater matrix (●) for *Pseudomonas putida* (A) and *Pseudokirchneriella subcapitata* test (B). (Mean \pm 95% Confidence Interval).

Despite treated water mixtures being notably less toxic than the single OFX, all profiles followed the same pattern. These data suggest that OFX is the main cause of aquatic toxicity and that the influence of ozonated by-products, especially those with potential biological activity (i.e., TP1-TP6), was almost negligible. It is interesting to note that the generation of easily assimilable organic matter [50], bicarbonate [51] and/or extra amounts of nitrate and phosphate [52] are the most likely cause of the remarkable stimulation observed for *P. putida* and *P. subcapitata* growth.

Despite the toxic effects towards *V. fischeri* initially decline in parallel with remaining OFX concentration afterwards, luminescence inhibition significantly increased at low ozone dosages (remaining OFX \approx 11 mg L⁻¹). Particularly, a steep increase was observed in the synthetic water matrix, reaching 50% for an ozone dosage of 39 mg L⁻¹. Part of this toxicity enhancement could be attributed to the formation of formaldehyde, whose concentration in synthetic water reached 1.0 mg L⁻¹ for an ozone dosage of 39 mg L⁻¹. This value is close to the EC₅₀ value of 8.4 mg L⁻¹ reported by Ricco et al. [53]. The occurrence of organic nitrogen compounds (1.85 mg L⁻¹ as organic nitrogen) could also represent a contribution to the total toxicity due to the high toxicity of some of them formed by the ozonation of the piperiziny group [54]. A similar toxicity trend was observed for *V. fischeri* in previous studies [37], [55] and [56]. Calza et al. [55] also suggested that the increase in the luminescence inhibition during photocatalytic treatment of OFX was not due to the initial TPs but to secondary products, namely piperazine and its derivatives and other degradation products, not detected by LC/MS. This fact highlighted the concern about the generation of secondary products with new and undesired new biological effects [40]. *V. fischeri* displayed the same toxicity pattern in the STP effluent although with lower toxicity, which is most likely due to the effect of the

wastewater matrix. The presence of other chemicals in wastewater may interfere with the mechanisms of action of OFX, minimizing the response or limiting the interaction with target bacterial receptors [57].

4. Conclusions

The continuous ozonation performances with short residence times attained total abatement of OFX in synthetic water and real STP effluent, but not totally mineralization is achieved. The water matrix has a strong influence on the ozone dose required for OFX removal and a given degree of mineralization.

The extent of mineralization was limited in both water matrices and a number of TPs appeared which suggested that reaction pathway include the oxidation of piperiziny and quinolone moieties. The degradation of the initial TPs gave rise to the formation and accumulation of final by-products such as carboxyl acids, aldehydes, nitrogen-containing organic compounds, and inorganic ions.

Although OFX is toxic both for target (*P. putida*) and non-target (*P. subcapitata*) organisms, ozonation completely removed its toxic effects, which implies that the generated by-products presented negligible toxicity.

Acknowledgements

This study has been financed by the Dirección General de Universidades e Investigación de la Comunidad de Madrid, Research Network S2013/MAE-2716. JBC thanks the Spanish Ministry of Education for a FPU grant (AP2008-00572).

Supplementary data

<http://www.sciencedirect.com/science/article/pii/S0304389415001806>.

References

- [1] E. van der Grinten, M.G. Pikkemaat, E.J. van den Brandhof, G.J. Stroomberg, M.H.S. Kraak, Comparing

- the sensitivity of algal, cyanobacterial and bacterial bioassays to different groups of antibiotics, *Chemosphere* 80 (2010) 1–6.
- [2] K. Kümmerer, Antibiotics in the aquatic environment—a review—part I, *Chemosphere* 75 (2009) 417–434.
- [3] D. Fatta-Kassinos, S. Meric, A. Nikolaou, Pharmaceutical residues in environmental waters and wastewater: current state of knowledge and future research, *Anal. Bioanal. Chem.* 399 (2011) 251–275.
- [4] K. Kümmerer, Antibiotics in the aquatic environment—a review—part II, *Chemosphere* 75 (2009) 435–441.
- [5] L. Rizzo, C. Manaia, C. Merlin, T. Schwartz, C. Dagot, M.C. Ploy, I. Michael, D. Fatta-Kassinos, Urban wastewater treatment plants as hotspots for antibiotic resistant bacteria and genes spread into the environment: a review, *Sci. Total Environ.* 447 (2013) 345–360.
- [6] T. Schwartz, W. Kohnen, B. Jansen, U. Obst, Detection of antibiotic-resistant bacteria and their genes in wastewater surface water and drinking water biofilms, *FEMS Microbiol. Ecol.* 43 (2003) 325–335.
- [7] Y. Yang, B. Li, S. Zou, H.H.P. Fang, T. Zhang, Fate of antibiotic resistance genes in sewage treatment plant revealed by metagenomic approach, *Water Res.* 62 (2014) 97–106.
- [8] R.A. Brain, K.R. Solomon, B.W. Brooks, Targets, effects and risks in aquatic plants exposed to veterinary antibiotics, in: K.L. Henderson, J.R. Coats (Eds.), *Veterinary Pharmaceuticals in the Environment*, American Chemical Society, Washington DC, 2009, pp. 169–189.
- [9] P. Sukul, M. Spiteller, Fluoroquinolone antibiotics in the environment, *Rev. Environ. Contam. Toxicol.* 191 (2007) 131–162.
- [10] B. Li, T. Zhang, Biodegradation and adsorption of antibiotics in the activated sludge process, *Environ. Sci. Technol.* 44 (2010) 3468–3473.
- [11] P. Verlicchi, M. Al Aukidy, E. Zambello, Occurrence of pharmaceutical compounds in urban wastewater: removal, mass load and environmental risk after a secondary treatment—a review, *Sci. Total Environ.* 429 (2012) 123–155.
- [12] P.A. Segura, M. François, C. Gagnon, S. Sauvé, Review of the occurrence of anti-infectives in contaminated wastewaters and natural and drinking waters, *Environ. Health Perspect.* 117 (2009) 675–684.
- [13] I. Michael, L. Rizzo, C.S. McArdell, C.M. Manaia, C. Merlin, T. Schwartz, C. Dagot, D. Fatta-Kassinos, Urban wastewater treatment plants as hotspots of the release of antibiotics in the environment: a review, *Water Res.* 47 (2013) 957–995.
- [14] T. Backhaus, M. Karlsson, Screening level mixture risk assessment of pharmaceuticals in STP effluents, *Water Res.* 49 (2014) 157–165.
- [15] K. Kümmerer, A. Al-Ahmad, V. Mersch-Sundermann, Biodegradability of some antibiotics, elimination of the genotoxicity and affection of wastewater bacteria in a simple test, *Chemosphere* 40 (2000) 701–710.
- [16] M. Isidori, M. Lavorgna, A. Nardelli, L. Pascarella, A. Parrella, Toxic and genotoxic evaluation of six antibiotics on non-target organisms, *Environ. Sci. Technol.* 346 (2005) 87–98.
- [17] T.A. Ternes, A. Joss, H. Siegrist, Peer reviewed: scrutinizing pharmaceuticals and personal care products in wastewater treatment, *Environ. Sci. Technol.* 38 (2004) 392A–399A.
- [18] R. Andreozzi, L. Campanella, B. Frayse, J. Garric, A. Gonnella, R. Lo Giudice, R. Marotta, G. Pinto, A. Pollio, Effects of advanced oxidation processes (AOPs) on the toxicity of a mixture of pharmaceuticals, *Water Sci. Technol.* 50 (2004) 23–28.
- [19] M.M. Huber, A. Göbel, A. Joss, N. Hermann, D. Löffler, C.S. McArdell, A. Ried, H. Siegrist, T.A. Ternes, U. von Gunten, Oxidation of pharmaceuticals during ozonation of municipal wastewater effluents: a pilot study, *Environ. Sci. Technol.* 39 (2005) 4290–4299.
- [20] R. Rosal, A. Rodríguez, J.A. Perdígón-Melón, A. Petre, E. García-Calvo, M.J. Gómez, A. Agüera, A.R. Fernández-Alba, Occurrence of emerging pollutants in urban wastewater and their removal through biological treatment followed by ozonation, *Water Res.* 44 (2010) 578–588.
- [21] A. Rodríguez, I. Muñoz, J.A. Perdígón-Melón, J.B. Carbajo, M.J. Martínez, A.R. Fernández-Alba, E. García-Calvo, R. Rosal, Environmental optimization of continuous flow ozonation for urban wastewater reclamation, *Sci. Total Environ.* 437 (2012) 68–75.
- [22] S.A. Tyrrell, S.R. Rippey, W.D. Watkins, Inactivation of bacterial and viral indicators in secondary sewage effluents, using chlorine and ozone, *Water Res.* 29 (1995) 2483–2490.
- [23] M.C. Dodd, Potential impacts of disinfection processes on elimination and deactivation of antibiotic resistance genes during water and wastewater treatment, *J. Environ. Monit.* 14 (2012) 1754–1771.
- [24] I.A. Katsoyiannis, S. Canonica, U. von Gunten, Efficiency and energy requirements for the transformation of organic micropollutants by ozone, O₃/H₂O₂ and UV/H₂O₂, *Water Res.* 45 (2011) 3811–3822.
- [25] M.C. Dodd, H.P.E. Kohler, U. von Gunten, Oxidation of antibacterial compounds by ozone and hydroxyl radical: elimination of biological activity during aqueous ozonation processes, *Environ. Sci. Technol.* 43 (2009) 2498–2504.
- [26] R.F. Dantas, S. Contreras, C. Sans, S. Esplugas, Sulfamethoxazole abatement by means of ozonation, *J. Hazard. Mater.* 150 (2008) 790–794.
- [27] K. Li, A. Yediler, M. Yang, S. Schulte-Hostede, M.H. Wong, Ozonation of oxytetracycline and toxicological assessment of its oxidation by-products, *Chemosphere* 72 (2008) 473–478.
- [28] M.M. Gómez-Ramos, M. Mezcuca, A. Agüera, A.R. Fernández-Alba, S. Gonzalo, A. Rodríguez, R. Rosal, Chemical and toxicological evolution of the antibiotic sulfamethoxazole under ozone treatment in water solution, *J. Hazard. Mater.* 192 (2011) 18–25.
- [29] L.J. Burrows, A.J. Stokes, J.R. West, C.F. Forster, A.D. Martin, Evaluation of different analytical methods for tracer studies in aeration lanes of activated sludge plants, *Water Res.* 33 (1999) 367–374.
- [30] J. Asenjo, J. Merchuck, *Bioreactor System Design*, Marcel Dekker Inc, New York, 1995.
- [31] ISO 11348-3, Water Quality—Determination of the Inhibitory Effect of Water Samples on the Light Emission of *Vibrio fischeri* (Luminescent Bacteria Test), International Standardization Organization, Geneva, 2007.
- [32] ISO 10712, Water Quality—*Pseudomonas putida* Growth Inhibition Test (Pseudomonas Cell Multiplication

- Inhibition Test), International Standardization Organization, Geneva, 1995.
- [33] OECD, Test No. 201, Freshwater Algae and Cyanobacteria. Growth Inhibition Test, OECD Guidelines for the Testing of Chemicals, Section 2, OECD Publishing, Paris, 2011.
- [34] Protoxkit F™, Freshwater Toxicity Test with a Ciliate Protozoan, Standard Operational Procedure, Creasel Deinze (1998).
- [35] G. Márquez, E.M. Rodríguez, F.J. Beltrán, P.M. Álvarez, Determination of rate constants for ozonation of ofloxacin in aqueous solution, *Ozone Sci. Eng.* 35 (2013) 186–195.
- [36] B. de Witte, H. van Langenhove, K. Hemelsoet, K. Demeestere, P. de Wispelaere, V. van Speybroeck, J. Dewulf, Levofloxacin ozonation in water: rate determining process parameters and reaction pathway elucidation, *Chemosphere* 76 (2009) 683–689.
- [37] N.H. El Najjar, A. Touffet, M. Deborde, R. Journal, N.K. Vel Leitner, Levofloxacin oxidation by ozone and hydroxyl radicals: kinetic study, transformation products and toxicity, *Chemosphere* 93 (2013) 604–611.
- [38] M.C. Dodd, M.O. Buffle, U. von Gunten, Oxidation of antibacterial molecules by aqueous ozone: moiety-specific reaction kinetics and application to ozone based wastewater treatment, *Environ. Sci. Technol.* 40 (2006) 1969–1977.
- [39] C. Liu, V. Nanaboina, G.V. Korshin, W. Jiang, Spectroscopic study of degradation products of ciprofloxacin, norfloxacin and lomefloxacin formed in ozonated wastewater, *Water Res.* 46 (2012) 5235–5246.
- [40] C. von Sonntag, U. von Gunten, *Chemistry of Ozone in Water and Wastewater Treatment: From Basic Principles to Applications*, IWA Publishing, London, 2012.
- [41] A.L. Petre, J.B. Carbajo, R. Rosal, E. García-Calvo, P. Letón, J.A. Perdígón-Melón, Influence of water matrix on copper-catalysed continuous ozonation and related ecotoxicity, *Appl. Catal. B: Environ.* 163 (2015) 233–240.
- [42] C. Liu, V. Nanaboina, G. Korshin, Spectroscopic study of the degradation of antibiotics and the generation of representative EfOM oxidation products in ozonated wastewater, *Chemosphere* 86 (2012) 774–782.
- [43] F. Muñoz, C. von Sonntag, The reactions of ozone with tertiary amines including the complexing agents nitrilotriacetic acid (NTA) and ethylenediaminetetraacetic acid (EDTA) in aqueous solution, *J. Chem. Soc. Perkin Trans. 2* (2000) 2029–2033.
- [44] J. Nawrocki, P. Andrzejewski, Nitrosamines and water, *J. Hazard. Mater.* 189 (2011) 1–18.
- [45] P. Xu, M.L. Janex, P. Savoye, A. Cockx, V. Lazarova, Wastewater disinfection by ozone: main parameters for process design, *Water Res.* 36 (2002) 1043–1055.
- [46] F. Sharif, J. Wang, P. Westerhoff, Transformation in bulk and trace organics during ozonation of wastewater, *Ozone Sci. Eng.* 34 (2012) 26–31.
- [47] T. Nöthe, H. Fahlenkamp, C. von Sonntag, Ozonation of wastewater: rate of ozone consumption and hydroxyl radical yield, *Environ. Sci. Technol.* 43 (2009) 5990–5995.
- [48] T. Backhaus, K. Froehner, R. Altenburger, L.H. Grimme, Toxicity testing with *Vibrio fischeri*: a comparison between the long term (24 h) and the short term (30 min) bioassay, *Chemosphere* 35 (1997) 2925–2938.
- [49] R. Alexy, *Antibiotika in Der Aquatischen Umwelt: Eintrag, Elimination Und Wirkung Auf Bakterien*, Ph.D. Dissertation, University of Freiburg, 2003.
- [50] P. Thayanukul, F. Kurisu, I. Kasuga, H. Furumai, Evaluation of microbial regrowth potential by assimilable organic carbon in various reclaimed water and distribution systems, *Water Res.* 47 (2013) 225–232.
- [51] H.C.H. Luzhøft, B. Halling-Sørensen, S.E. Jørgensen, Algal toxicity of antibacterial agents applied in Danish fish farming, *Arch. Environ. Contam. Toxicol.* 36 (1999) 1–6.
- [52] S.Y. Selivanovskaya, N.Y. Stepanove, Y.-T. Hung, Bioassay of industrial waste pollutants, in: L.K. Wang, Y.T. Hung, H.H. Lo, C. Yapikackis (Eds.), *Handbook of Industrial and Hazardous Wastes Treatment*, Marcel Dekker Inc., New York, 2004, pp. 15–61.
- [53] G. Ricco, M.C. Tomei, R. Ramadori, G. Laera, Toxicity assessment of common xenobiotic compounds on municipal activated sludge: comparison between respirometry and Microtox®, *Water Res.* 38 (2004) 2103–2110.
- [54] D. Calamari, R. Da Gasso, S. Galassi, A. Provini, M. Vighi, Biodegradation and toxicity of selected amines on aquatic organisms, *Chemosphere* 9 (1980) 753–762.
- [55] P. Calza, C. Medana, F. Carbone, V. Giancotti, C. Baiocchi, Characterization of intermediate compounds formed upon photoinduced degradation of quinolones by high-performance liquid chromatography/high-resolution multiple-stage mass spectrometry, *Rapid Commun. Mass Spectrom.* 22 (2008) 1533–1552.
- [56] M.I. Vasquez, M. Garcia-Käufer, E. Hapeshi, J. Menz, K. Kostarelos, D. Fatta-Kassinos, K. Kümmerer, Chronic ecotoxic effects to *Pseudomonas putida* and *Vibrio fischeri*, and cytostatic and genotoxic effects to the hepatoma cell line (HepG2) of ofloxacin photo(catalytically) treated solutions, *Sci. Total Environ.* 450–451 (450) (2013) 356–365.
- [57] M.D. Hernando, S. De Vettori, M.J. Martínez-Bueno, A.R. Fernández-Alba, Toxicity evaluation with *Vibrio fischeri* test of organic chemicals used in aquaculture, *Chemosphere* 68 (2007) 724–730.

Supplementary Material

Continuous ozonation treatment of ofloxacin: Transformation products, water matrix effect and aquatic toxicity

José B. Carbajo¹, Alice L. Petre^{1,2}, Roberto Rosal^{1,2}, Sonia Herrera^{2,3}, Pedro Letón^{1,2}, Eloy García-Calvo^{1,2}, Amadeo R. Fernández-Alba^{2,3}, José A. Perdigón-Melón^{1,*}

- 1 Departamento de Ingeniería Química, Universidad de Alcalá, E-28871, Alcalá de Henares, Madrid, Spain
- 2 Advanced Study Institute of Madrid, IMDEA-Agua, Parque Científico Tecnológico, E-28805 Alcalá de Henares, Spain
- 3 Department of Chemistry and Physics, University of Almería, E-04120 Almería, Spain

* Corresponding author: ja.perdigon@uah.es

Contents:

Detailed experimental set-up, analytical methods and bioassays protocols; Main physico-chemical parameters of STP effluent (Table S1); Accurate mass measurement of product ions of ofloxacin (OFX) and its transformation products (TPs) determined by LC/ESI-QTOF-MS; Evolution of OFX in the synthetic water matrix without and with *t*-butanol (30 mM) at different levels of consumed ozone (Fig. S1); Evolution of DOC, consumed and dissolved ozone at different ozone dosages in the synthetic water matrix and STP effluent (Fig. S2). Concentration-response curve of OFX (Fig. S3).

EXPERIMENTAL SET-UP

The experiments were carried out in a cylindrical reactor made of Pyrex (internal diameter of 6.0 cm and working height of 51 cm) with a total working volume of 1.44 L, which operated in continuous co-current mode (Scheme 1). The retention time distribution curve yielded an average retention time of 10.3 min. The reactor modelling using the continuous stirred tank reactor (CSTR) in series model determined an equivalent value of 1.13 tanks, indicating that the bubble column can reasonably approach a perfect CSTR. Water flow rate was 142 mL·min⁻¹ (Gilmont rotameter) and gas flow was 390 mL·min⁻¹ (Aalborg mass flow controller) with different inlet ozone concentrations (Anseros ozone generator COM-AD-02). Inlet and outlet ozone gas concentrations (Anseros NDUV ozone GM-PRO analyser), dissolved ozone (Mettler Toledo-Thomton dissolved ozone sensor), pH and temperature (EasyfermPlus VP 120 Hamilton pH sensor) were continuously monitored (Keithley 2700 Data Acquisition System) and recorded in a computer.

ANALYTICAL METHODS

OFX concentration was performed by HPLC, Agilent 1200, with reversed-phase C18 analytical column (Phenomenex Luna SCX, 250 × 4.6 mm, 5 μm) and operated at a flow rate

of $0.5 \text{ mL} \cdot \text{min}^{-1}$. An isocratic method, with 30% acetonitrile and 70% ultrapure water with 0.1 M phosphoric acid and 10 mM ammonium acetate mobile phase, was employed with detection of OFX at $\lambda = 294 \text{ nm}$. The structural elucidation of TPs was carried out using a hybrid quadrupole time-of-flight mass spectrometer TripleTOF 5600 system (AB SCIEX) with an ESI (electrospray ionization) source coupled to an Agilent 1200 Series HPLC system (LC/ESI-QTOF-MS). The ion source parameters were: Ion Spray Voltage Floating (ISVF), 5500 V; Temperature (TEM), 550°C; Curtain Gas (CUR), 25 (arbitrary units) and Ion Source Gas (GS1 and GS2) at 35 psi and 40 psi, respectively. The MS was operated in full scan TOF-MS and MS/MS mode through information dependent acquisition (IDA) in a single run analysis. In addition to the discriminative information based on mass accuracy of the molecular ions acquired in TOF-MS, MS/MS mode was used for the characterization of the TPs. The declustering potential (DP) and collision energy (CE) were 70 V and 10 V in the full scan TOF-MS experiment. The LC analysis was performed with a reversed-phase C18 analytical column (Agilent Zorbax Eclipse XDB, $50 \times 4.6 \text{ mm}$, $1.8 \mu\text{m}$). Mobile phases A and B were, respectively, acetonitrile and HPLC-grade water with 0.1% formic acid. A linear gradient was set from 10% to 100% of A in 11 min, and then maintained at 100% for 5 min. Data acquisition and processing were carried out using Analyst[®] TF 1.5 and PeakView[™] (AB SCIEX) software.

Dissolved Organic Carbon (DOC) was determined using a TOC-V_{CSH} Shimadzu TOC analyzer. Carboxylic acids were measured by a Dionex DX120 Ion Chromatograph with a conductivity detector. Oxalic and mesoxalic acid concentrations were analyzed by IonPac AS9-HC analytical column ($4 \times 250 \text{ mm}$) with ASRS-Ultra suppressor whereas, acetic and formic acid concentrations were measured using an IonPac ICE analytical column ($9 \times 250 \text{ mm}$) with AMMS-ICE II suppressor. Inorganic ions were determined by means of a Metrohm 861 Advance Compact IC with conductivity detector; a Metrosep A Supp 7-250 analytical column was used in anion analysis while, a Metrosep C3 column was used in cation analysis. Formaldehyde was measured photometrically using the acetylacetone method (Hach-Lange LCK 325).

AQUATIC TOXICITY BIOASSAYS PROCEDURE

Vibrio fischeri acute test measure the decrease in bioluminescence induced in the cell metabolism. The bioassay was performed according to ISO 11348-3 standard protocol [31] using the commercial BioFix[®]Lumi test (*V. fischeri*, NRRL-B 11177 from Macherey-Nagel, Germany). Bioluminescence was measured at $15 \pm 1^\circ\text{C}$ after 30 min in 96-well white polypropylene microplate by a Fluoroskan Ascent FL microplate luminometer (Thermo Scientific). *Pseudomonas putida* test determine the inhibitory effect of a substance on the bacteria (*P. putida*, NCIB 9494 from CECT, Spain) by means of cell growth inhibition. The bioassay was performed according to ISO guideline 10712 [32]. Bacterial culture was exposed to test solutions at $23 \pm 1^\circ\text{C}$ for 16 h in 10 mL glass incubation vials which were constantly shaken in the dark. The cell growth was determined by optical density ($\lambda = 600 \text{ nm}$) in 96-well clear polypropylene microplate using a Rayto RT-2100C microplate reader.

Algal growth inhibition test was carried out following the procedure described in the European Guideline OECD TG (Guideline) 201, using *Pseudokirchneriella subcapitata* open system [33]. The algal stock culture for inoculation was taken from commercial test system Algaltokit F[™] (MicroBioTest Inc., Belgium). The cells of *P. subcapitata* were exposed to tested water samples at $23 \pm 1^\circ\text{C}$ for 72 h in 10 mL glass incubation vials which were

constantly shaken and illuminated in a chamber ($\sim 100 \mu\text{mol foton}\cdot\text{m}^{-2}\cdot\text{s}^{-1}$). Algal biomass was measured daily by chlorophyll-*a* content, whose extraction was carried out as following: 50 μL culture samples were transferred to a 96-well black polypropylene microplate, 200 μL of ethanol was added to each well and the plate was shaken for 3 h in the dark. Thereafter the fluorescence was measured using a Fluoroskan Ascent FL microplate fluorometer (Excitation 450 nm, Emission 672 nm) from Thermo Scientific.

Finally, growth inhibition assay with the ciliate protozoan *Tetrahymena thermophila* was carried out according to the Standard Operational Procedure Guidelines of Protoxkit FTM [34]. The test is based on the turnover of substrate into ciliate biomass. Substrate and reconstitution medium were purchased from MicroBioTest Inc. (Belgium) whereas *T. thermophila* (SB 210) was kindly supplied by D. Cassidy-Hanley (Tetrahymena Stock Center, USA). Ciliates were incubated with water samples and food suspension in test vessels at $30\pm 1^\circ\text{C}$ for 24 h in the dark. Growth inhibition was determined on the basis of turbidity changes (OD at $\lambda = 440 \text{ nm}$), at the beginning and at the end of the test.

ZnSO₄·7H₂O for *V. fischeri* test, 3,5-dichlorophenol for *P. putida* and K₂Cr₂O₇ for the rest of the bioassays were used as reference substances in order to check each test procedures. Three independent experiments with duplicate samples were carried out to ensure reproducibility. All aquatic toxicity data are expressed as mean \pm 95% confidence interval and data analysis were performed using a nonlinear-regression sigmoidal dose-response curve model provided in the GraphPad Prism 6.0 software (GraphPad software Inc., San Diego, USA).

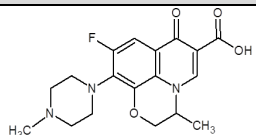
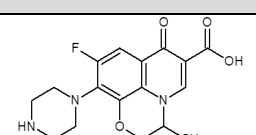
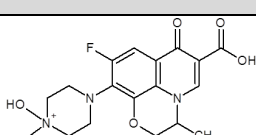
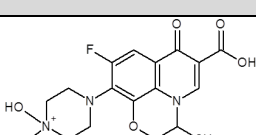
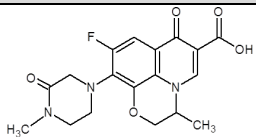
Table S1. Main physico-chemical parameters of STP effluent.

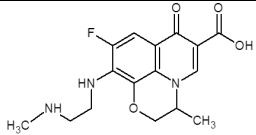
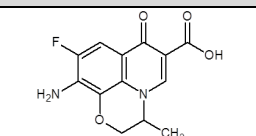
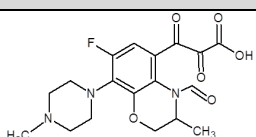
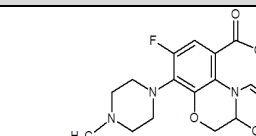
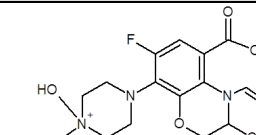
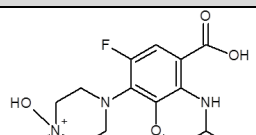
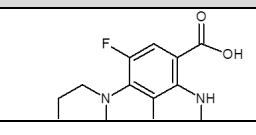
pH	7.4	Na ⁺ (mg·L ⁻¹)	65.	Cr (μg L ⁻¹)	0.36
Conductivity (μS·cm ⁻¹)	750	NH ₄ ⁺ (mg·L ⁻¹)	4.1	Ni (μg L ⁻¹)	12
TSS (mg·L ⁻¹)	11	K ⁺ (mg·L ⁻¹)	15	Cu (μg L ⁻¹)	12
Turbidity (NTU)	7.0	Mg ²⁺ (mg·L ⁻¹)	18	Zn (μg L ⁻¹)	63
COD (mg·L ⁻¹)	28	Ca ²⁺ (mg·L ⁻¹)	52	As (μg L ⁻¹)	9.2
DOC (mg·L ⁻¹)	8.4	Cl ⁻ (mg·L ⁻¹)	86	Se (μg L ⁻¹)	0.29
BOD ₅ (mg·L ⁻¹)	6.0	NO ₂ ⁻ (mg·L ⁻¹)	5.6	Cd (μg L ⁻¹)	ND
BOD ₅ /COD	0.22	NO ₃ ⁻ (mg·L ⁻¹)	59	Hg (μg L ⁻¹)	ND
SUVA ₂₅₄ * (L·mg C ⁻¹ m ⁻¹)	2.6	PO ₄ ³⁻ (mg·L ⁻¹)	3.3	Pb(μg L ⁻¹)	ND
Alkalinity (mg CaCO ₃ ·L ⁻¹)	138	SO ₄ ²⁻ (mg·L ⁻¹)	81	Cr (μg L ⁻¹)	0.36

*Specific Ultraviolet Absorption at 254 nm

ND non-detected

Table S2. Accurate mass measurement of product ions of ofloxacin (OFX) and its transformation products (TPs) determined by LC/ESI-QTOF-MS.

Compound	R _t (min)	Elemental formula	Mass (<i>m/z</i>)		Error		Proposed structure
			Theoretical	Experimental	ppm	DBE	
OFX	4.170	C ₁₈ H ₂₁ FN ₃ O ₄ ⁺	362.1511	362.1518	2.0	9.5	
		C ₁₇ H ₂₁ FN ₃ O ₂ ⁺	318.1612	318.1608	-1.2	8.5	
		C ₁₄ H ₁₄ FN ₂ O ₂ ⁺	261.1034	261.1025	-3.4	8.5	
		C ₁₁ H ₁₀ FN ₂ O ₂ ⁺	221.0721	221.0713	-3.5	7.5	
TP1	4.150	C ₁₇ H ₁₉ FN ₃ O ₄ ⁺	348.1354	348.1367	3.7	9.5	
		C ₁₇ H ₁₇ FN ₃ O ₃ ⁺	330.1249	330.1256	2.3	9.5	
		C ₁₆ H ₁₉ FN ₃ O ₂ ⁺	304.1456	304.1468	3.9	8.5	
		C ₁₆ H ₁₈ N ₃ O ₂ ⁺	284.1394	284.1404	3.7	8.5	
		C ₁₄ H ₁₄ FN ₂ O ₂ ⁺	261.1034	261.1052	6.9	8.5	
TP2	4.550	C ₁₈ H ₂₁ FN ₃ O ₅ ⁺	378.1460	378.1471	2.9	9.5	
		C ₁₈ H ₂₀ FN ₃ O ₄ ⁺	361.1432	361.1421	-3.2	9.5	
		C ₁₈ H ₁₉ FN ₃ O ₄ ⁺	360.1354	360.1372	5.0	9.5	
		C ₁₇ H ₂₁ FN ₃ O ₃ ⁺	334.1562	334.1579	5.2	8.5	
		C ₁₇ H ₂₁ N ₂ O ₄ ⁺	317.1496	317.1530	11	8.5	
TP3	3.940	C ₁₈ H ₂₁ FN ₃ O ₆ ⁺	394.1409	394.1419	2.6	9.5	
		C ₁₈ H ₁₉ N ₂ O ₆ ⁺	359.1238	359.1285	13	7.5	
		C ₁₇ H ₁₉ N ₂ O ₄ ⁺	315.1339	315.1378	12	8.5	
		C ₁₅ H ₁₂ FN ₂ O ₃ ⁺	287.0827	287.0835	3.0	10.5	
		C ₁₃ H ₁₂ FN ₂ O ₂ ⁺	247.0877	247.0907	12	7.5	
TP4	3.435	C ₁₈ H ₁₉ FN ₃ O ₅ ⁺	376.1303	376.1323	5.3	10.5	
		C ₁₈ H ₁₇ FN ₃ O ₄ ⁺	358.1198	358.1205	2.1	11.5	
		C ₁₅ H ₁₂ FN ₂ O ₃ ⁺	287.0826	287.0825	-0.3	10.5	
		C ₁₄ H ₁₄ FN ₂ O ₂ ⁺	261.1034	261.1036	0.8	8.5	
TP5	4.117	C ₁₆ H ₁₉ FN ₃ O ₄ ⁺	336.1354	336.1346	-0.4	8.5	

		$C_{16}H_{17}FN_3O_3^+$	318.1249	318.1248	-0.2	9.5	
		$C_{13}H_{10}FN_2O_3^+$	298.1186	298.1188	0.7	10.5	
		$C_{13}H_{10}FN_2O_3^+$	261.0670	261.0692	8.4	9.5	
TP6	5.953	$C_{13}H_{12}FN_2O_4^+$	279.0775	279.0780	1.8	8.5	
		$C_{13}H_{10}FN_2O_3^+$	261.0670	261.0674	1.6	8.5	
		$C_{10}H_5FN_2O_3^+$	220.0279	220.0284	2.4	7.5	
		$C_{10}H_4FN_2O_3^+$	219.0200	219.0209	4.1	7.5	
TP7	4.533	$C_{18}H_{21}FN_3O_6^+$	394.1409	394.1426	4.3	9.5	
		$C_{15}H_{14}FN_2O_4^+$	305.0932	305.0944	3.9	9.5	
		$C_{14}H_{14}FN_2O_2^+$	261.1034	261.1059	9.6	8.5	
		$C_{13}H_{12}FN_2O_2^+$	247.0877	247.0884	2.8	6.5	
TP8	0.953	$C_{16}H_{21}FN_3O_4^+$	338.1511	338.1537	7.7	7.5	
		$C_{15}H_{21}FN_3O_3^+$	310.1562	310.1577	5.0	6.5	
		$C_{15}H_{19}FN_3O_2^+$	292.1456	292.1462	2.1	7.5	
		$C_{12}H_{12}FN_2O_2^+$	235.0877	235.0888	4.7	7.5	
TP9	2.322	$C_{16}H_{21}FN_3O_5^+$	354.1460	354.1469	2.6	7.5	
		$C_{16}H_{20}FN_3O_4^+$	337.1432	337.1453	6.1	7.5	
		$C_{15}H_{20}FN_3O_3^+$	309.1483	309.1466	-5.6	6.5	
		$C_{15}H_{19}N_3O_3^+$	289.1421	289.1443	7.6	5.5	
TP10	4.585	$C_{15}H_{21}FN_3O_4^+$	326.1511	326.1523	3.8	6.5	
		$C_{15}H_{20}FN_3O_3^+$	309.1483	309.1480	-1.0	6.5	
		$C_{15}H_{19}N_3O_3^+$	289.1421	289.1417	-1.3	5.5	
		$C_{14}H_{14}FN_2O_2^+$	261.1034	261.1078	17	8.5	
		$C_{11}H_{10}FN_2O_2^+$	221.0721	221.0713	-3.5	7.5	
TP11	1.878	$C_{14}H_{19}FN_3O_4^+$	312.1354	312.1364	3.2	6.5	
		$C_{13}H_{17}FN_3O_2^+$	266.1299	266.1285	-5.4	5.5	
		$C_{12}H_{12}FN_2O^+$	219.0928	219.0917	-5.1	4.5	

		$C_{11}H_{14}FN_2O^+$	209.1085	209.1099	6.8	5.5	
TP12	4.441	$C_{16}H_{19}FN_3O_4^+$	336.1354	336.1350	-1.2	8.5	
		$C_{16}H_{18}FN_3O_3^+$	319.1327	319.1329	0.7	8.5	
		$C_{15}H_{18}FN_3O_2^+$	291.1378	291.1395	6.0	6.5	
		$C_{14}H_{15}FN_3O_2^+$	276.1143	276.1142	-0.3	8.5	
		$C_{13}H_{10}FN_2O_3^+$	261.0670	261.0692	8.4	9.5	

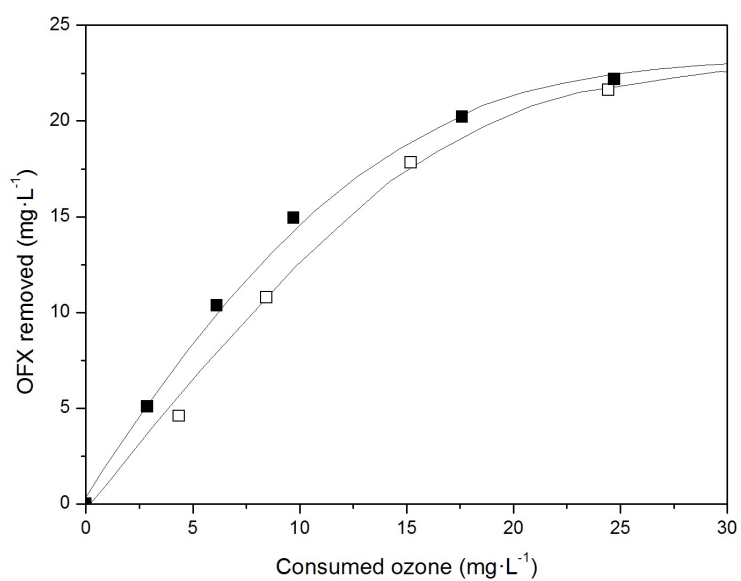
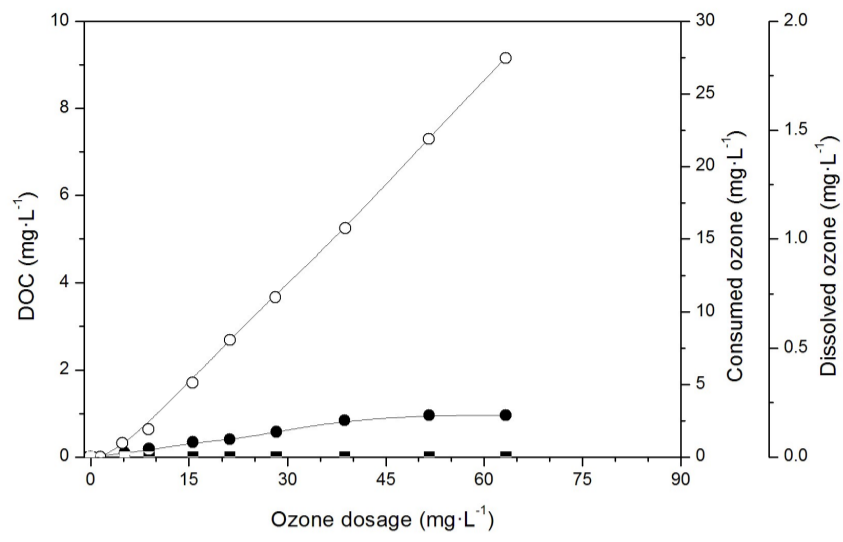


Fig. S1. Evolution of ofloxacin (OFX) in the synthetic water matrix without (■) and with *t*-butanol (30 mM) (□) at different levels of consumed ozone.

(A)



(B)

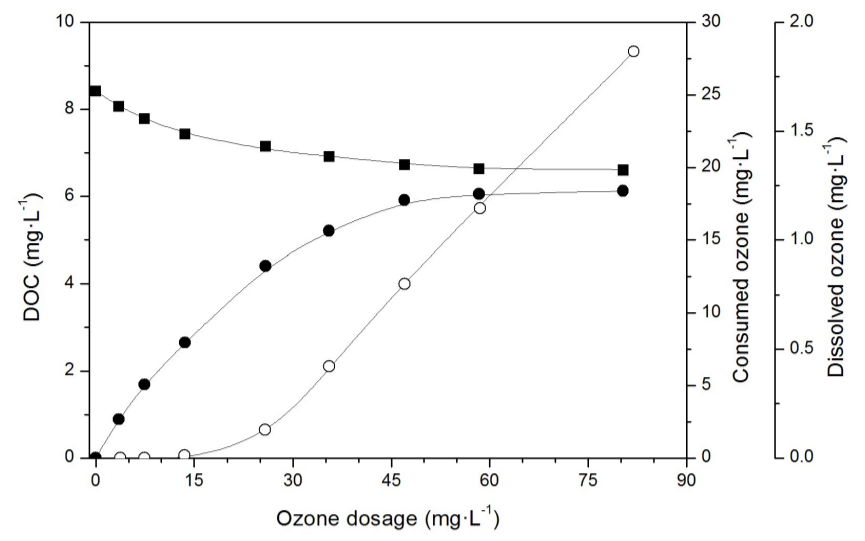


Fig. S2. Evolution of DOC (■), consumed (●) and dissolved ozone (○) at different ozone dosages in the synthetic water matrix (A) and STP effluent (B).

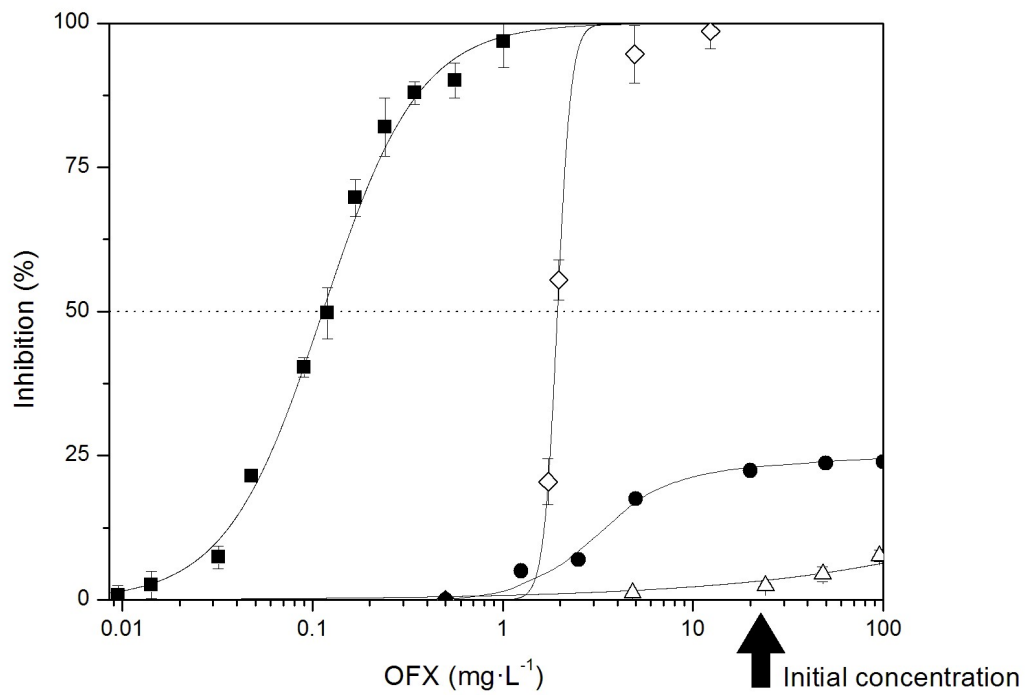


Fig. S3. Concentration-response curve of ofloxacin (OFX) for *V. fischeri* (●), *P. putida* (■), *P. subcapitata* (◇) and *T. thermophila* (Δ) test (mean ± 95% confidence interval). Black arrow represents the initial OFX concentration in spiked waters (22 mg·L⁻¹).